Eur Radiol (2013) 23:1812–1821
DOI 10.1007/s00330-013-2788-z

CARDIAC

Diagnostic accuracy of combined coronary angiography and adenosine stress myocardial perfusion imaging using 320-detector computed tomography: pilot study

Arthur Nasis · Brian S. Ko · Michael C. Leung · Paul R. Antonis · Dee Nandurkar · Dennis T. Wong · Leo Kyi · James D. Cameron · John M. Troupis · Ian T. Meredith · Sujith K. Seneviratne

Received: 16 October 2012 / Revised: 23 December 2012 / Accepted: 6 January 2013 / Published online: 21 February 2013

Abstract
Objectives To determine the diagnostic accuracy of combined 320-detector row computed tomography coronary angiography (CTA) and adenosine stress CT myocardial perfusion imaging (CTP) in detecting perfusion abnormalities caused by obstructive coronary artery disease (CAD).
Methods Twenty patients with suspected CAD who underwent initial investigation with single-photon-emission computed tomography myocardial perfusion imaging (SPECT-MPI) were recruited and underwent prospectively-gated 320-detector CTA/CTP and invasive angiography. Two blinded cardiologists evaluated invasive angiography images quantitatively (QCA). A blinded nuclear physician analysed SPECT-MPI images for fixed and reversible perfusion defects. Two blinded cardiologists assessed CTA/CTP studies qualitatively. Vessels/territories with both >50 % stenosis on QCA and corresponding perfusion defect on SPECT-MPI were defined as ischaemic and formed the reference standard.
Results All patients completed the CTA/CTP protocol with diagnostic image quality. Of 60 vessels/territories, 17 (28 %) were ischaemic according to QCA/SPECT-MPI criteria. Sensitivity, specificity, PPV, NPV and area under the ROC curve for CTA/CTP was 94 %, 98 %, 94 %, 98 % and 0.96 ($P<0.001$) on a per-vessel/territory basis. Mean CTA/CTP radiation dose was 9.2±7.4 mSv compared with 13.2± 2.2 mSv for SPECT-MPI ($P<0.001$).
Conclusions Combined 320-detector CTA/CTP is accurate in identifying obstructive CAD causing perfusion abnormalities compared with combined QCA/SPECT-MPI, achieved with lower radiation dose than SPECT-MPI.
Key Points
- *Advances in CT technology provides comprehensive anatomical and functional cardiac information.*
- *Combined 320-detector CTA/adenosine-stress CTP is feasible with excellent image quality.*
- *Combined CTA/CTP is accurate in identifying myocardial ischaemia compared with QCA/SPECT-MPI.*
- *Combined CTA/CTP results in lower patient radiation exposure than SPECT-MPI.*
- *CTA/CTP may become an established imaging technique for suspected CAD.*

Keywords Coronary artery disease · Multidetector computed tomography · Adenosine stress myocardial perfusion · Single-photon emission computed tomography · Myocardial ischaemia

Abbreviations

CAD	Coronary artery disease
CTA	Computed tomography coronary angiography
CTP	Computed tomography stress myocardial perfusion imaging

A. Nasis · B. S. Ko · M. C. Leung · P. R. Antonis · D. T. Wong · L. Kyi · J. D. Cameron · I. T. Meredith · S. K. Seneviratne (✉)
Monash Cardiovascular Research Centre, Monash Heart, Department of Medicine Monash Medical Centre (MMC), Southern Health and Monash University, Melbourne, Australia
e-mail: Sujith.Seneviratne@southernhealth.org.au

D. Nandurkar · J. M. Troupis
Department of Diagnostic Imaging, MMC, Southern Health, Melbourne, Australia

SPECT-MPI	Single-photon emission computed tomography myocardial perfusion imaging
QCA	Quantitative coronary angiography
SRS	Summed rest score
SSS	Summed stress score
LAD	Left anterior descending
LCx	Left circumflex
RCA	Right coronary artery
PPV	Positive predictive value
NPV	Negative predictive value
ROC	Receiver-operator characteristic

Introduction

The presence of myocardial ischaemia is an important risk factor for adverse clinical outcomes in patients with coronary artery disease (CAD) [1, 2]. Furthermore, revascularisation of ischaemia-inducing coronary stenoses improves patient outcomes and functional status [3–6]. Whilst computed tomography coronary angiography (CTA) allows accurate visualisation of coronary plaque [7] and assessment of coronary stenosis with high diagnostic accuracy [8–10], the ability of CTA to accurately predict coronary stenoses that result in myocardial ischaemia is limited by low specificity and positive predictive value (PPV) [11, 12]. Recent advances in multidetector CT have broadened its clinical utility to include a comprehensive evaluation of patients with suspected CAD in a non-invasive manner to assess myocardial perfusion in addition to visualisation of coronary atherosclerotic plaque and luminal stenosis in a single examination. Furthermore, the recent introduction of wide-area detector 320-detector-row systems offers significant advantages over previous-generation partial-volume coverage systems, including complete cardiac coverage in a single heartbeat, permitting dynamic imaging without stair-step artefacts and temporal contrast uniformity during the first pass of contrast medium with lower patient radiation exposure [13, 14].

Most studies published to date have evaluated myocardial CT perfusion imaging (CTP) using 64-detector-row technology and have demonstrated diagnostic accuracy comparable to single-photon emission computed tomography myocardial perfusion imaging (SPECT-MPI) [15–18], with limited data currently available regarding the diagnostic accuracy of combined CTA/CTP using 320-detector technology. We therefore sought to determine the diagnostic accuracy of combined 320-detector CTA and adenosine stress CTP in detecting perfusion abnormalities caused by obstructive CAD in symptomatic patients with suspected CAD, as well as to evaluate whether 320-detector CTP, when added to CTA, provides incremental diagnostic accuracy to CTA alone in detecting myocardial ischaemia.

Materials and methods

Study population

We prospectively recruited 20 consecutive symptomatic patients with suspected CAD who underwent initial investigation with SPECT-MPI and subsequent invasive angiography within 30 days. Exclusion criteria included age <40 years, atrial fibrillation, second- or third-degree atrioventricular block, renal insufficiency (eGFR <60 ml/min/1.73 m^2), bronchospastic lung disease, critical aortic stenosis and contraindications to iodinated contrast medium. All participants were scheduled for combined cardiac CTA/CTP within 7 days of invasive angiography. The institutional human research ethics committee approved the study protocol and all participants signed written informed consent.

Combined CT angiography and myocardial stress perfusion image acquisition

Before imaging, blood pressure and heart rate were measured and intravenous access was obtained in the right and left antecubital veins for iodinated contrast medium and adenosine administration. Oral metoprolol was administered as required, aiming for a resting heart rate below 60 beats per minute (bpm). No other premedication was administered. The combined CTA/CTP protocol involved rest CTA followed by adenosine stress CTP (Fig. 1).

Rest CT coronary angiography

CT was performed on a commercially available 320-slice CT system (AquilionOne, Toshiba Medical Systems, Tokyo, Japan). After biplanar scout images, a bolus of 55 ml of 100 % iohexol (56.6 g/75 ml; Omnipaque 350) was injected at a flow rate of 5 ml/s, followed by 20 ml of a 30:70 mixture of contrast medium and saline, respectively, followed by 30 ml saline. Imaging was triggered in the arterial phase using automated contrast bolus tracking, with a region of interest placed in the descending aorta, and automatically triggered at 300 Hounsfield units (HU). An axial imaging technique was used with slice collimation 0.5 mm and gantry rotation time 350 ms. The number of detectors selected, and hence the volume coverage, was determined by cardiac size seen on scout images (either 16 cm using 320 detectors or 14 cm using 280 detectors). Exposure parameters include an X-ray tube potential of 120 kV and effective tube current of 300–500 mA, based on vendor specifications and determined by the patient's body mass index. All acquisitions were performed with prospective electrocardiogram-triggering using a 70–80 % phase window. When images were acquired at heart rates <65 bpm, imaging was completed within a single R–R

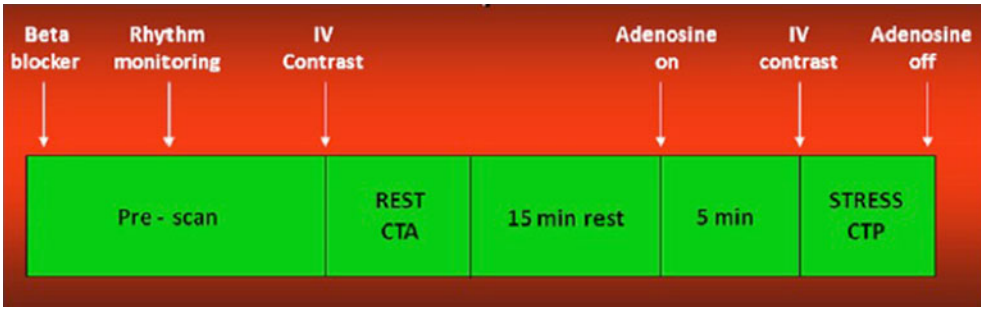

Fig. 1 Combined CTA/CTP imaging protocol. After patient preparation, rest CTA is performed followed by adenosine stress CTP. Both acquisitions are performed with prospective electrocardiogram-triggering. Detailed explanation of the protocol is provided in the "Materials and methods" section

interval utilising a 180° segment, providing an effective temporal resolution of 175 ms. When images were acquired at a heart rate >65 bpm, data segments from two consecutive beats were used for multi-segment reconstruction with improved temporal resolution of 87 ms.

Stress myocardial CT perfusion imaging

Twenty minutes after acquisition of the resting images, intravenous adenosine infusion was commenced at 140 μg/kg/min, with continuous electrocardiogram monitoring in the presence of a cardiologist. Five minutes into the adenosine infusion, iodinated contrast medium was administered as per the resting images. CTP imaging was performed with prospective electrocardiogram-triggering using a 70–95 % phase window over one or two consecutive heart beats, depending on the heart rate, as outlined above. Exposure parameters were the same as for the resting images.

Nuclear stress testing and invasive angiography

All SPECT-MPI examinations were performed using technetium-99 m sestamibi according to standard institution protocols with symptom-limited treadmill exercise or pharmacological (dipyridamole or adenosine) stress. Examinations were performed using a 1-day stress-rest protocol, unless patients weighed >120 kg, who underwent a 2-day stress-rest protocol. An adequate stress test was defined as either achieving >85 % of the maximum predicted heart rate, any test using a pharmacological stress agent or the patient developing ischaemic-sounding chest pain during exercise testing. The total sestamibi dose for the stress and rest protocols was individualised to the patient weight, ranging between 1.0 and 1.3 Gbq of Tc-99 m sestamibi. Images were acquired on a 'Cardio MDIII' camera system (Philips Healthcare, Eindhoven, The Netherlands) . Attenuation correction was not used for any patient <120 kg; instead, images were obtained in supine and prone positions for both female and male patients to correct for diaphragmatic attenuation. Patients weighing >120 kg were imaged on the 'Precedence' camera (Philips Healthcare, Eindhoven, The Netherlands), where attenuation correction was used using a CT source. Invasive angiography was performed in all patients via the femoral or radial approach using standard orthogonal views according to standard institution protocols.

Image processing and interpretation

Combined CT angiography and myocardial stress perfusion

Electrocardiogram-gated resting CTA datasets were reconstructed automatically to overlapping 0.5-mm slices in 0.25-mm intervals at 75 % of the R–R cycle length. Additional reconstruction windows were constructed after examination of initial datasets if motion or noise artefacts were present. Stress CTP datasets were reconstructed at 80 % of the R-R interval, with further reconstructions at 3 % intervals, as required to optimise detection of beam hardening and motion artefacts. The phase with the least cardiac motion was then selected and a short-axis average multiplanar reconstruction series was created using 5-mm-thick slices. Images were displayed using a narrow window-level display (width 300 HU, level 150 HU).

Anonymised CT datasets were transferred to a post-processing workstation (Vitrea Fx 6.2, Vital Images, MN, USA). Images were analysed by consensus by two experienced CT readers (S.S., M.L.), who were unaware of the clinical data and blinded to the results of quantitative coronary angiography (QCA) and SPECT-MPI. CTA images were interpreted first followed by CTP assessment in a combined fashion as recommended by CTP interpretation guidelines [19]. CTA images were interpreted using the 17-segment modified American Heart Association model [20]. All available coronary segments were visually assessed, regardless of size, for degree of luminal stenosis and a vessel was considered significant if there was ≥1 segment that was non-evaluable or with a ≥50 % luminal stenosis. In addition, a luminal diameter stenosis threshold of ≥70 % was used in secondary analyses. CTP images were interpreted using the 17-segment model recommended by the American College of Cardiology/American Heart Association/American Society of Nuclear Cardiology [21]. Each of the 17 segments was visually assessed for the presence or absence of a perfusion defect. Perfusion defects were classified as transmural (≥50 %

myocardial wall thickness) or non-transmural (<50 % wall thickness). Reversibility was defined as 0=none, 1=minimal, 2=partial, 3=complete. In addition, for each dataset image quality was graded according to a three-point scale: 1=suboptimal, 2=good, 3=excellent.

SPECT-MPI imaging

A single experienced nuclear medicine physician (D.N.), unaware of clinical data and blinded to the results of QCA and CTA/CTP, assessed SPECT-MPI images using the same 17-segment myocardial model [18]. A semi-quantitative visual assessment of myocardial perfusion was performed using a four-point scale: 0=normal, 1=mild reduction of radioisotope uptake, 2=moderate reduction of radioisotope uptake, 3=severe reduction of radioisotope uptake. Reversibility was also determined. The summed rest score (SRS) and summed stress score (SSS) were calculated as the sum of the scores on the rest and stress images, respectively.

Quantitative coronary angiography

Quantitative coronary angiography was performed on all coronary arteries ≥1.5 mm in diameter using a semi-automated edge detection system (CMS Version 6, Medis Medical Imaging Systems, Ridgefield, CT, USA) by two interventional cardiologists (P.A., B.K.) who were blinded to SPECT-MPI and CT findings using the same 17-segment modified American Heart Association model [20]. Similar to CTA, a vessel was classified as containing significant stenosis if maximal vessel diameter reduction by QCA was ≥50 % in any segment in any angiographic view. In addition, a maximal vessel diameter reduction ≥70 % was used in secondary analyses.

Matching myocardial perfusion segments to vascular territories

In order to correctly associate the 17 myocardial segments with the subtended vascular territory on both SPECT-MPI and CTP, we used CTA to determine the following, as we have previously described [13]:

1. Whether the left circumflex (LCx) or right coronary artery (RCA) supplied the inferior wall
2. Whether the anterolateral wall was supplied by the left anterior descending artery (LAD) via a diagonal vessel overlying the anterolateral wall
3. Whether the inferolateral wall was supplied by the RCA using an overlying right posterolateral branch
4. Whether the distal LAD wrapped around the apex to supply the distal inferior wall
5. Whether the LAD septal perforator supplied the inferior septum

Reference standard and radiation exposure

The primary reference standard was obstructive CAD (stenosis ≥50 % in any vessel on QCA) with an associated reversible perfusion defect on SPECT-MPI in the corresponding vascular territory, as outlined above. Secondary analyses were also conducted against the following reference standards:

1. Stenosis ≥70 % in any vessel on QCA with an associated reversible perfusion defect on SPECT-MPI in the corresponding vascular territory
2. Obstructive CAD (stenosis ≥50 %) in any vessel on QCA alone
3. Obstructive CAD (stenosis ≥70 %) in any vessel on QCA alone

Effective radiation dose for CTA, CTP and combined CTA/CTP imaging was calculated by multiplying the dose–length product reported by the system by a constant (k=0.014 mSv/mGy/cm) according to standard methodology [22]. Estimates of effective radiation dose for SPECT-MPI were calculated by converting total megabecquerels to millisieverts.

Statistical analysis

Continuous data are expressed as mean ± standard deviation. Categorical data are expressed as percentage frequency. Sensitivity, specificity, PPV and negative predictive value (NPV) were calculated to determine the diagnostic accuracy of combined CTA/CTP as well as CTA alone to detect perfusion abnormalities caused by obstructive CAD on a per patient and vessel territory basis. Precision of these parameters was expressed as 95 % confidence intervals that were calculated according to the efficient score method [23]. The area under the receiver-operator characteristic (ROC) curve was calculated and reported with 95 % confidence intervals and compared with an area under the curve under the null hypothesis of 0.5 [24]. Areas under the ROC curves for different diagnostic approaches were compared with one other using the approach of DeLong et al. [25]. In addition, the incremental value of CTP to CTA in the identification of perfusion abnormalities caused by obstructive CAD was evaluated using the integrated discrimination improvement index (IDI) as described by Pencina et al. [26]. Difference in radiation exposure between techniques was compared using the Wilcoxon signed-rank test. Analysis was performed on an 'intention-to-diagnose' basis, denoting that coronary segments on CTA that were non-diagnostic because of artefact were considered to contain obstructive CAD (≥50 % luminal narrowing), reflecting real world practice. A P value <0.05 was considered statistically significant. Data were analysed using Stata 12.1 (StataCorp, College Station, TX, USA).

Results

Patient population

Twenty patients (average age 66.4±10.4 years, 65 % male) were recruited and all patients successfully completed the full CTA/CTP protocol with no adverse events. The median interval between invasive angiography and CTA/CTP was 3 days (interquartile range 2–5 days), and the median interval between SPECT-MPI and CTA/CTP was 18 days (interquartile range 9–29 days). There were no clinical events between initial SPECT-MPI and CTA/CTP in any patient. Patient characteristics are outlined in Table 1.

Quantitative coronary angiography findings

On QCA, seven (35 %) patients had ≥50 % stenosis and five (25 %) patients had ≥70 % stenosis in at least one coronary vessel. Single-vessel disease was present in two patients (10 %) and triple-vessel disease in five patients (25 %). On a per vessel basis, 17 (28 %) vessels studied had a ≥50 % stenosis (7 LAD, 5 LCx and 5 RCA) and 15 (25 %) had a ≥70 % stenosis (5 LAD, 5 LCx and 5 RCA). No significant left main stenosis was present.

Table 1 Patient characteristics

Characteristic	Value
Age (years), mean±SD (range)	66.4±10.4 (42–81)
Male sex, *n* (%)	13 (65 %)
Height (cm), mean±SD	169±14
Weight (kg), mean±SD	83.1±15
Body mass index (kg/m^2), mean±SD (range)	29.2±5.3 (18–40)
Hypertension[a], *n* (%)	14 (70)
Hypercholesterolaemia[b], *n* (%)	13 (65)
Current smoker, *n* (%)	2 (10)
Ex-smoker, *n* (%)	7 (35)
Diabetes, *n* (%)	6 (30)
Family history IHD, *n* (%)	7 (35)
Obesity[c], *n* (%)	5 (25)
Creatinine (mmol/l), mean±SD	85.4±19.3
Medication, *n* (%)	
Aspirin	6 (30)
Clopidogrel	1 (5)
Beta-blocker	4 (20)
ACE inhibitor	5 (25)
Angiotensin receptor blocker	2 (10)
Statin	5 (25)
Calcium channel blocker	2 (10)

SD standard deviation, *IHD* ischaemic heart disease, *ACE* angiotensin converting enzyme

[a] Blood pressure >140/90 mmHg or treatment for hypertension

[b] Total cholesterol >180 mg/dl or treatment for hypercholesterolaemia

[c] Body mass index >30 kg/m^2

SPECT-MPI findings

On SPECT-MPI, 16 patients (85 %) and 32 vascular territories (53 %) demonstrated perfusion abnormalities during stress. Of the 16 patients with perfusion abnormalities on SPECT-MPI, 12 (75 %) had reversible ischaemia and 4 (25 %) had fixed perfusion deficits. Of the 32 vascular territories with perfusion abnormalities on SPECT-MPI, 15 (47 %) were fully reversible, 10 (31 %) were partially reversible and 7 (22 %) were fixed. The mean (range) SSS and SRS was 9.3±8.8 (0–30) and 4.0±3.8 (0–12) respectively.

Combined CT angiography and myocardial stress perfusion findings

All patients successfully completed the CT protocol with diagnostic image quality (60 vessels/vascular territories available for analysis). Eleven (55 %) patients required oral metoprolol for heart rate control. Table 2 outlines the CTA and CTP imaging parameters and image quality assessment.

On CTA, nine patients (45 %) and 24 vessels (40 %) were found to have at least one segment containing ≥50 % stenosis. Of nine patients with at least one segment containing ≥50 % stenosis, one (5 %) had single-vessel disease, one (5 %) had double-vessel disease and seven (35 %) had triple-vessel disease. When using at least one segment containing ≥70 %

Table 2 CT acquisition parameters and image quality

Parameter	CTA	CTP
Heart rate (bpm)[a], mean±SD	54.7±11.2	63.0±12.3
Sinus rhythm[a], *n* (%)	20 (100)	20 (100)
Blood pressure[a], mean±SD		
Systolic	150.2±18.4	156.5±19.1
Diastolic	76.5±11.0	76.9±11.4
Gantry rotations[a], *n* (%)		
1	19 (95)	16 (80)
2	1 (5)	4 (20)
Tube voltage (kV), mean±SD	120±0	120±0
Tube current (mA), mean±SD	478.7±49.7	436.5±70.1
Dose–length product (mGy-cm), mean±SD	316±247	341±275
Radiation exposure (mSv), mean±SD	4.4±3.5	4.8±3.9
Image quality (using subjective three-point scale), mean±SD	2.5±0.8	2.5±0.8

CTA computed tomography angiography, *CTP* computed tomography perfusion imaging

[a] At time of CT image acquisition

stenosis as a cut-off for obstructive CAD, nine patients (45 %) and 21 vessels (35 %) were found to have at least one segment containing obstructive stenosis. Of nine patients with at least one segment containing ≥70 % stenosis, one (5 %) had single-vessel disease, four (20 %) had double-vessel disease and four (20 %) had triple-vessel disease. Two vessels (3 %) overall had at least one non-evaluable segment, both secondary to heavy calcification, and were considered to contain obstructive CAD.

On adenosine stress CTP, eight patients (40 %) and 17 vascular territories (28 %) demonstrated perfusion abnormalities (example shown in Fig. 2). In patients with perfusion defects on CTP, two (10 %) had a defect involving one vessel territory, one (5 %) had defects involving two vessel territories and four (20 %) had defects involving three vessel territories. Of these, eight (13 %) were located in the LAD territory, four (7 %) in LCx territory and five (8 %) in the RCA territory. Nine (53 %) were transmural defects and eight (47 %) were non-transmural. All vascular territories with perfusion abnormalities identified on CTP were reversible using resting CTA for comparison, with six (35 %) partially reversible, and 11 (65 %) completely reversible.

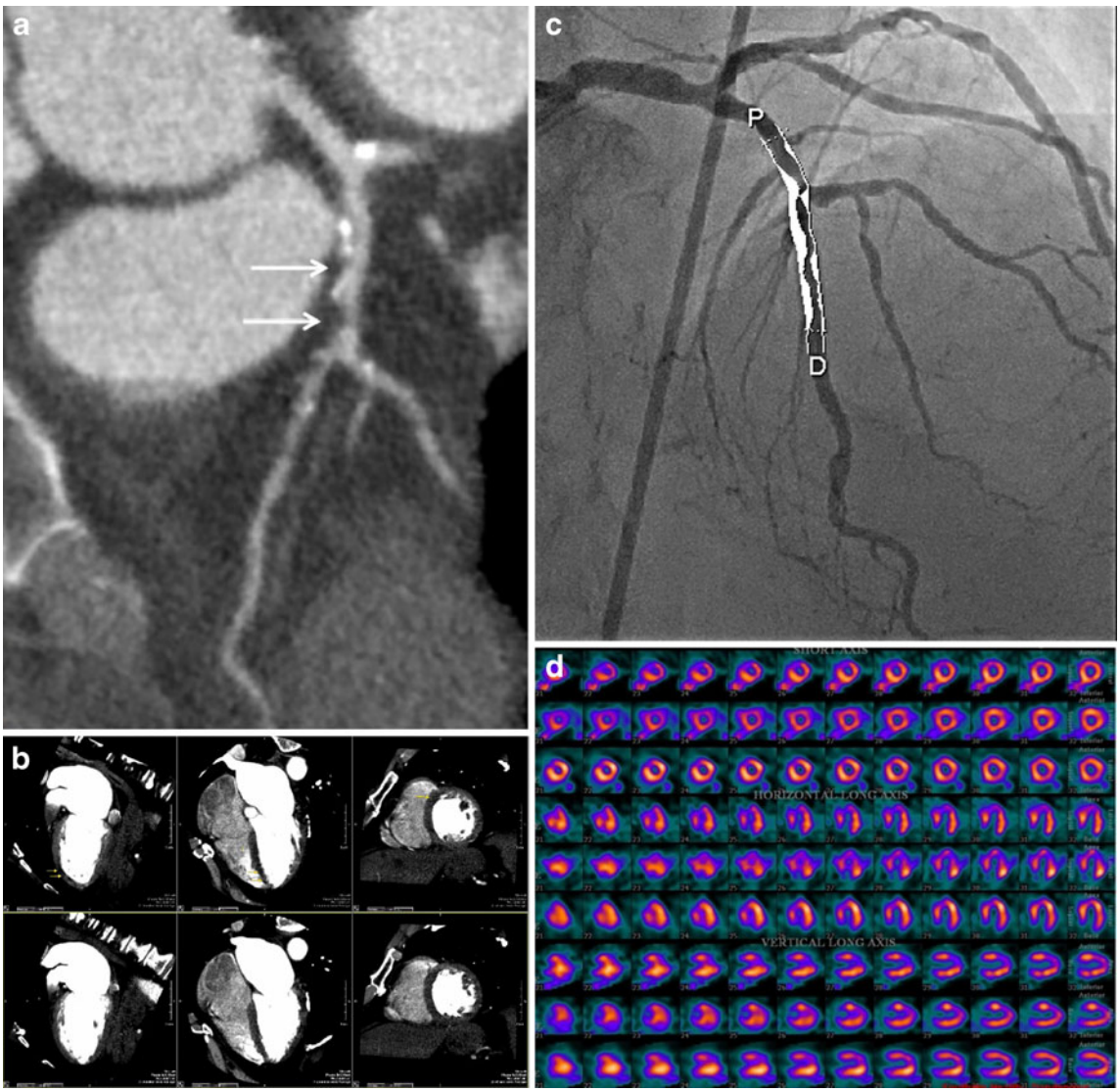

Fig. 2 Demonstration of obstructive coronary stenosis causing perfusion abnormality demonstrated by all techniques. A 66-year-old man with exertional chest pain. **a** CTA demonstrates mixed plaque resulting in >70 % stenosis in the mid left anterior descending (LAD) artery (*white arrows*). **b** Adenosine stress CTP shows perfusion defects in the mid-anteroseptal, apical septal and apical anterior myocardial segments (*yellow arrows*, *upper panels*) with normal perfusion on resting images (*lower panels*), indicating reversible LAD territory ischaemia. **c** Invasive angiography in the cranial left anterior oblique view demonstrates a long segment of severe stenosis in the mid LAD between proximal (*P*) and distal (*D*) reference points (77 % by QCA). **d** Short axis, horizontal and vertical long-axis SPECT-MPI images show a reversible perfusion defect in the mid anterior and apical segments

Diagnostic accuracy of combined CT angiography and myocardial stress perfusion imaging

Diagnostic accuracy of CTA for the detection of perfusion abnormalities caused by obstructive CAD before and after perfusion analysis, with obstructive CAD defined as both ≥50 % and ≥70 % luminal stenosis at QCA with an associated reversible perfusion defect on SPECT-MPI in the corresponding vascular territory, are summarised in Table 3. With a threshold of ≥50 % luminal stenosis used to define obstructive CAD, mean values of the diagnostic accuracy of combined CTA/CTP on a per vascular territory analysis were: sensitivity, 94 % (95 % confidence interval, 69–86 %); specificity, 98 % (86–100 %); PPV, 94 % (69–99 %); NPV, 98 % (86–100 %); and mean values of the diagnostic accuracy of CTA alone on a per vascular territory analysis were: sensitivity, 100 % (77–100 %); specificity, 84 % (69–93 %); PPV, 71 % (49–86 %); NPV, 100 % (88–100 %). The area under the ROC curve increased from 0.92 (0.86–0.97) to 0.96 (0.90–1.0) upon addition of CTP analysis findings (P=0.3). With a threshold of ≥70 % luminal stenosis used to define obstructive CAD, mean values of the diagnostic accuracy of combined CTA/CTP on a per vascular territory analysis were: sensitivity, 79 % (49–94 %); specificity, 91 % (78–97 %); PPV, 73 % (45–91 %) ; NPV, 93 % (81–98 %); and mean values of the diagnostic accuracy of CTA alone on a per vascular territory analysis were: sensitivity, 86 % (56–97 %); specificity, 80 % (66–90 %); PPV, 57 % (37–77 %); NPV, 95 % (81–99 %). The area under the ROC curve increased from 0.83 (0.72–0.94) to 0.85 (0.73–0.97) upon addition of CTP analysis findings (P=0.7). As CTA and CTP images were interpreted in a combined fashion (i.e. CTP abnormalities were only considered in vascular territories subtended by vessels with ≥50 % stenosis on CTA), the diagnostic accuracy of CTP alone was not analysed.

The incremental diagnostic accuracy of analysing CTP in addition to CTA for the identification of perfusion abnormalities caused by obstructive CAD as indicated by combined QCA/SPECT-MPI was evaluated using the IDI. At a

Table 3 Diagnostic accuracy of combined CTA/CTP and CTA alone compared with reference standard of obstructive coronary stenosis (QCA ≥50 % and ≥70 %) and reversible defect on SPECT-MPI

	Per patient analysis	Per vessel analysis
Combined CTA stenosis ≥50 % and perfusion defect on CTP		
Sensitivity (%)	100 (56–100), 7/7	94 (69–86), 16/17
Specificity (%)	92 (62–99), 12/13	98 (86–100), 42/43
PPV (%)	88 (47–99), 7/8	94 (69–99), 16/17
NPV (%)	100 (70–100), 12/12	98 (86–100), 42/43
AUC	0.96 (0.87–1.0), P<0.001	0.96 (0.90–1.0), P<0.001
Accuracy (%)	95, 19/20	97, 58/60
CTA stenosis ≥50 % alone		
Sensitivity (%)	100 (56–100), 7/7	100 (77–100), 17/17
Specificity (%)	85 (54–97), 11/13	84 (69–93), 36/43
PPV (%)	78 (40–96), 7/9	71 (49–86), 17/24
NPV (%)	100 (67–100), 11/12	100 (88–100), 36/36
AUC	0.92 (0.80–1.0), P=0.002	0.92 (0.86–0.97), P<0.001
Accuracy (%)	90, 18/20	88, 53/60
Combined CTA stenosis ≥70 % and perfusion defect on CTP		
Sensitivity (%)	100 (46–100), 5/5	79 (49–94), 11/14
Specificity (%)	80 (51–95), 12/15	91 (78–97), 42/46
PPV (%)	63 (26–90), 5/8	73 (45–91), 11/15
NPV (%)	100 (70–100), 12/12	93 (81–98), 42/45
AUC	0.90 (0.76–1.0), P=0.009	0.85 (0.73–0.97), P<0.001
Accuracy (%)	85, 17/20	88, 53/60
CTA stenosis ≥70 % alone		
Sensitivity (%)	100 (46–100), 5/5	86 (56–97), 12/14
Specificity (%)	73 (45–91), 11/15	80 (66–90), 37/46
PPV (%)	56 (23–85), 5/9	57 (34–77), 12/21
NPV (%)	100 (68–100), 11/11	95 (81–99), 37/39
AUC	0.87 (0.71–1.0), P=0.016	0.83 (0.72–0.97), P<0.001
Accuracy (%)	80, 16/20	82, 49/60

CTA computed tomography angiography, *CTP* computed tomography stress myocardial perfusion imaging, *QCA* quantitative coronary angiography, *SPECT-MPI* single photon emission computed tomography myocardial perfusion imaging, *PPV* positive predictive value, *NPV* negative predictive value; *AUC* area under the receiver-operator characteristic curve; *values in parentheses* represent 95 % confidence intervals

stenosis threshold of 50 %, the IDI for CTP in addition to CTA was 0.64 ($P<0.001$), and using a stenosis threshold of 70 %, the IDI for CTP in addition to CTA was 0.13 ($P=0.006$). These results suggest incremental diagnostic accuracy in the performance of CTP in addition to CTA findings, particularly using a stenosis threshold of 50 %.

Radiation exposure

The mean radiation exposures for CTA, CTP and combined CTA/CTP assessment were 4.4±3.5, 4.8±3.9 and 9.2±7.4 mSv respectively. The mean radiation exposure for SPECT-MPI was 13.2±2.2 mSv, significantly higher than combined CTA/CTP ($P<0.001$).

Discussion

This study demonstrates that in patients with suspected CAD, combined 320-detector CTA/CTP has high diagnostic accuracy in detecting obstructive CAD causing perfusion abnormalities on both per-patient and per-vascular territory analyses when compared with combined QCA/SPECT-MPI, at both >50 % and >70 % stenosis thresholds. In addition, there may be incremental value in adding CTP to CTA alone in the identification of perfusion abnormalities caused by obstructive CAD, particularly with improved specificity and PPV, which are the main limitations on the overall diagnostic accuracy of CTA alone. This is further supported by IDI analysis, particularly at the >50 % stenosis threshold. Furthermore, combined CTA/CTP can be performed using prospective electrocardiogram-triggering with a lower total radiation dose than SPECT-MPI, currently the most frequently used technique for detecting myocardial ischaemia.

To our knowledge, this is the first study to report the diagnostic accuracy of combined 320-detector CTA/CTP compared with QCA and SPECT-MPI as the reference standard. Two previous studies have assessed the diagnostic accuracy of 320-detector CTP; however, the first compared CTP with fractional flow reserve in high-risk patients considered for coronary revascularisation [13], and the second compared CTP with SPECT-MPI alone with no invasive comparison except in a small subset [27]. Both of these studies showed a moderate to high overall diagnostic accuracy of CTP with areas under the ROC curve of 0.67 and 0.92, respectively. These studies are also the only two to utilise a CT protocol with prospective electrocardiogram-triggering, displaying slightly higher total radiation doses of 11.3 mSv and 13.8 mSv.

Multiple earlier single-centre studies have been performed that have examined the diagnostic accuracy of CTP utilising older generation 64-detector [15–18], 128-detector [28–30] and 256-detector [16] technologies. These have reported sensitivity ranging from 81 % to 96 % and specificity from 72 % to 98 % compared with QCA and/or SPECT. A 320-detector CT offers improved cranio-caudal coverage compared with earlier generation systems, and enables anatomical and perfusion imaging of the entire heart at a single time point with temporal contrast uniformity during the first pass of contrast medium without misregistration artefacts. Furthermore, these earlier studies all used retrospective electrocardiogram-triggering with resultant higher patient radiation exposure up to 21.6 mSv [16]. Our total radiation dose of 9.2 mSv was considerably lower than those of previous studies [15–18, 28–30] and significantly lower than SPECT-MPI in our cohort, demonstrating the feasibility of a prospective electrocardiogram-triggered acquisition protocol with the advantage over SPECT-MPI of providing both anatomical and functional assessment in a single examination. However in the future, we may see innovatively designed dedicated cardiac nuclear cameras with cadmium-zinc-telluride solid-state detectors that have the potential for increased sensitivity and reduced patient radiation exposure [31].

The majority of previous studies evaluating the feasibility and diagnostic accuracy of CTP have evaluated patients with known CAD [28–30] or awaiting revascularisation [13]. AHA/ACC appropriateness criteria suggest that this population is not suitable for assessment with CTA, which is usually performed for the assessment of low-to-intermediate risk chest pain [32]. Accordingly we evaluated the diagnostic accuracy of CTA/CTP in symptomatic patients with suspected CAD and excluded patients with known CAD. Furthermore, unlike most previous studies, our protocol involved rest CTA followed by adenosine stress CTP (Fig. 1). This is because this sequence reflects the potential role of combined CTA/CTP in the clinical assessment of suspected CAD, whereby non-obstructive stenosis on CTA would obviate the need for CTP. Our results support this approach with CTA alone having a sensitivity and NPV of 100 % in excluding myocardial ischaemia. In addition, initial rest imaging is associated with higher sensitivity for the detection of previous myocardial infarction than if performed after CTP [33].

Whilst the overall diagnostic accuracy of CTA/CTP was high, there were occasional false-positive and false-negative results. False-positive territories were the result of artefacts, most commonly beam hardening or motion that is associated with increased heart rate driven by adenosine-induced hyperaemia. False-negatives were either due to the small size of the perfusion defect or overlying motion artefacts that precluded accurate assessment of particular territories. Future technological advances in CT systems to further improve diagnostic accuracy of CTP are anticipated such as improvement in temporal resolution to reduce motion artefacts, improved spatial resolution to delineate normal from hypoperfused myocardium and improved beam hardening correction algorithms.

The high diagnostic accuracy of CTA/CTP demonstrated in this study supports the use of this technique to evaluate

patients with suspected CAD for both coronary stenosis and myocardial perfusion in a single examination. A suggested protocol would involve initial CTA in all referred patients, with those found to have at least one obstructive (>50 %) stenosis on CTA proceeding to CTP to assess for the presence of myocardial ischaemia. If CTP excluded the presence of ischaemia, this would avoid the need for downstream ICA, which in isolation has limited ability to detect myocardial ischaemia [34]. In this way, combined CTA/CTP could be used as a 'gatekeeper' to ICA in a similar way to stress echocardiography, magnetic resonance perfusion and SPECT-MPI [35, 36], with the advantage of providing both anatomical and functional information in a single examination. Finally, the novel technique of non-invasive fractional flow reserve computed from CT may also be used for this purpose in a similar patient population in the future, with data from a recent multicentre trial showing that this technique results in improved diagnostic accuracy and discrimination compared with CTA alone for the diagnosis of haemodynamically significant CAD [37].

There were some limitations to the study. This is a single-centre study with results needing confirmation in larger multicentre studies such as the planned CORE-320 study [38]. Furthermore, analysis of the incremental diagnostic accuracy of combined CTA/CTP over CTA alone for the detection of myocardial ischaemia should be considered pilot data as they are limited by the relatively small number of patients with wide confidence intervals and as such are underpowered to exclude a true difference on comparison of areas under the ROC curves. The IDI results do, however, suggest incremental diagnostic accuracy, particularly using a stenosis threshold of 50 %, and provide an estimate of spread that may be used in the design of future prospective studies. Finally, beta-blockers were administered in 55 % of patients. Whilst beta-blockers may mask perfusion defects in exercise and dobutamine nuclear perfusion imaging, effects upon vasodilator perfusion imaging have been inconsistent [39–41] and the effect on CTP imaging is unknown.

In conclusion, in patients with suspected CAD, combined 320-detector CTA/CTP has high diagnostic accuracy in detecting obstructive CAD causing perfusion abnormalities compared with combined QCA/SPECT-MPI, and is performed with a lower radiation dose than SPECT-MPI. In addition, combined CTA/CTP may provide incremental diagnostic accuracy over CTA alone for the detection of myocardial ischaemia. If validated in larger multicentre studies, this technique may become an established clinical technique for investigating patients with suspected CAD.

Funding Sources Dr Arthur Nasis currently holds research scholarships from the National Health and Medical Research Council (NHMRC), the National Heart Foundation of Australia and the Southern Health Senior Medical Staff Association.

References

1. Beller G, Zaret B (2000) Contributions of nuclear cardiology to diagnosis and prognosis of patients with coronary artery disease. Circulation 101:1465–1478
2. Shaw L, Iskandrian A (2004) Prognostic value of gated myocardial perfusion SPECT. J Nucl Cardiol 11:171–185
3. Davies R, Goldberg A, Forman S et al (1997) Asymptomatic Cardiac Ischemia Pilot (ACIP) study two-year follow-up: outcomes of patients randomized to initial strategies of medical therapy versus revascularization. Circulation 95:2037–2043
4. Erne P, Schoenenberger A, Burckhardt D et al (2007) Effects of percutaneous coronary interventions in silent ischemia after myocardial infarction: the SWISSI II randomized controlled trial. JAMA 297:1985–1991
5. Hachamovitch R, Hayes S, Friedman J et al (2003) Comparison of the short-term survival benefit associated with revascularization compared with medical therapy in patients with no prior coronary artery disease undergoing stress myocardial perfusion single photon emission computed tomography. Circulation 107:2900–2907
6. Shaw L, Berman D, Maron D et al (2008) Optimal medical therapy with or without percutaneous coronary intervention to reduce ischemic burden: results from the Clinical Outcomes Utilizing Revascularization and Aggressive Drug Evaluation (COURAGE) trial nuclear substudy. Circulation 117:1283–1291
7. Schuhbäck A, Marwan M, Gauss S et al (2012) Interobserver agreement for the detection of atherosclerotic plaque in coronary CT angiography: comparison of two low-dose image acquisition protocols with standard retrospectively ECG-gated reconstruction. Eur Radiol 22:1529–1536
8. Budoff M, Dowe D, Jollis J et al (2008) Diagnostic performance of 64-multidetector row coronary computed tomographic angiography for evaluation of coronary artery stenosis in individuals without known coronary artery disease: results from the prospective multicenter ACCURACY (Assessment by Coronary Computed Tomographic Angiography of Individuals Undergoing Invasive Coronary Angiography) trial. J Am Coll Cardiol 52:1724–1732
9. Dewey M, Zimmermann E, Deissenrieder F et al (2009) Noninvasive coronary angiography by 320-row computed tomography with lower radiation exposure and maintained diagnostic accuracy: comparison of results with cardiac catheterization in a head-to-head pilot investigation. Circulation 120:867–875
10. Neefjes L, Rossi A, Genders T et al (2012) Diagnostic accuracy of 128-slice dual-source CT coronary angiography: a randomized comparison of different acquisition protocols. Eur Radiol 23:614-622
11. Rispler S, Keidar Z, Ghersin E et al (2007) Integrated single-photon emission computed tomography and computed tomography coronary angiography for the assessment of hemodynamically significant coronary artery lesions. J Am Coll Cardiol 49:1059–1067
12. Hacker M, Jakobs T, Hack N et al (2007) Sixty-four slice spiral CT angiography does not predict the functional relevance of coronary artery stenoses in patients with stable angina. Eur J Nucl Med Mol Imaging 34:4–10
13. Ko B, Cameron J, Meredith I et al (2012) Computed tomography stress myocardial perfusion imaging in patients considered for revascularization: a comparison with fractional flow reserve. Eur Heart J 33:67–77
14. Gervaise A, Osemont B, Lecocq S et al (2012) CT image quality improvement using adaptive iterative dose reduction with wide-volume acquisition on 320-detector CT. Eur Radiol 22:295–301
15. Blankstein R, Shturman L, Rogers I et al (2009) Adenosine-induced stress myocardial perfusion imaging using dual-source cardiac computed tomography. J Am Coll Cardiol 54:1072–1084

16. George R, Arbab-Zadeh A, Miller J et al (2009) Adenosine stress 64- and 256-row detector computed tomography angiography and perfusion imaging: a pilot study evaluating the transmural extent of perfusion abnormalities to predict atherosclerosis causing myocardial ischemia. Circ Cardiovasc Imaging 2:174–182
17. Okada D, Ghoshhajra B, Blankstein R et al (2010) Direct comparison of rest and adenosine stress myocardial perfusion CT with rest and stress SPECT. J Nucl Cardiol 17:27–37
18. Rocha-Filho J, Blankstein R, Shturman L et al (2010) Incremental value of adenosine-induced stress myocardial perfusion imaging with dual-source CT at cardiac CT angiography. Radiology 254:410–419
19. Mehra V, Valdiviezo C, Arbab-Zadeh A et al (2011) A stepwise approach to the visual interpretation of CT-based myocardial perfusion. J Cardiovasc Comput Tomogr 5:357–369
20. Austen W, Edwards J, Frye R et al (1975) A reporting system on patients evaluated for coronary artery disease. Report of the Ad Hoc Committee for Grading of Coronary Artery Disease, Council on Cardiovascular Surgery. Circulation 51:5–40
21. Cerqueira M, Weissman N, Dilsizian V et al (2002) Standardized myocardial segmentation and nomenclature for tomographic imaging of the heart: a statement for healthcare professionals from the Cardiac Imaging Committee of the Council on Clinical Cardiology of the American Heart Association. Circulation 105:539–542
22. Shrimpton P, Hillier M, Lewis M, Dunn M (2006) National survey of doses from CT in the UK: 2003. Br J Radiol 79:968–980
23. Newcombe R (1998) Two-sided confidence intervals for the single proportion: comparison of seven methods. Stat Med 17:857–872
24. Zweig M, Campbell G (1993) Receiver-operating characteristic (ROC) plots: a fundamental evaluation tool in clinical medicine. Clin Chem 39:561–577
25. DeLong E, DeLong D, Clarke-Pearson D (1988) Comparing the areas under two or more correlated receiver operating characteristic curves: a nonparametric approach. Biometrics 44:837–845
26. Pencina M, D'Agostino R Sr, D'Agostino R Jr, Vasan R (2008) Evaluating the added predictive ability of a new marker: from area under the ROC curve to reclassification and beyond. Stat Med 27:157–172, discussion 207–12
27. George R, Arbab-Zadeh A, Miller J et al (2012) Computed tomography myocardial perfusion imaging with 320-row detector computed tomography accurately detects myocardial ischemia in patients with obstructive coronary artery disease. Circ Cardiovasc Imaging 5:333–340
28. Bamberg F, Becker A, Schwarz F et al (2011) Detection of hemodynamically significant coronary artery stenosis: incremental diagnostic value of dynamic CT-based myocardial perfusion imaging. Radiology 260:689–698
29. Bastarrika G, Ramos-Duran L, Rosenblum M, Kang D, Rowe G, Schoepf U (2010) Adenosine-stress dynamic myocardial CT perfusion imaging: initial clinical experience. Invest Radiol 45:306–313
30. Feuchtner G, Goetti R, Plass A et al (2011) Adenosine stress high-pitch 128-slice dual-source myocardial computed tomography perfusion for imaging of reversible myocardial ischemia: comparison with magnetic resonance imaging. Circ Cardiovasc Imaging 4:540–549
31. Garcia E, Faber T, Esteves F (2011) Cardiac dedicated ultrafast SPECT cameras: new designs and clinical implications. J Nucl Med 52:210–217
32. Taylor A, Cerqueira M, Hodgson J et al (2010) ACCF/SCCT/ACR/AHA/ASE/ASNC/NASCI/SCAI/SCMR 2010 Appropriate use criteria for Cardiac Computed Tomography. A Report of the American College of Cardiology Foundation Appropriate Use Criteria Task Force, the Society of Cardiovascular Computed Tomography, the American College of Radiology, the American Heart Association, the American Society of Echocardiography, the American Society of Nuclear Cardiology, the North American Society for Cardiovascular Imaging, the Society for Cardiovascular Angiography and Interventions, and the Society for Cardiovascular Magnetic Resonance. J Cardiovasc Comput Tomogr 4:e1–e33
33. Techasith T, Cury R (2011) Stress myocardial CT perfusion: an update and future perspective. JACC Cardiovasc Imaging 4:905–916
34. Tonino P, Fearon W, De Bruyne B et al (2010) Angiographic versus functional severity of coronary artery stenoses in the FAME study fractional flow reserve versus angiography in multivessel evaluation. J Am Coll Cardiol 55:2816–2821
35. Jung P, Rieber J, Stork S et al (2008) Effect of contrast application on interpretability and diagnostic value of dobutamine stress echocardiography in patients with intermediate coronary lesions: comparison with myocardial fractional flow reserve. Eur Heart J 29:2536–2543
36. Gaemperli O, Husmann L, Schepis T et al (2009) Coronary CT angiography and myocardial perfusion imaging to detect flow-limiting stenoses: a potential gatekeeper for coronary revascularization? Eur Heart J 30:2921–2929
37. Min J, Leipsic J, Pencina M et al (2012) Diagnostic accuracy of fractional flow reserve from anatomic CT angiography. JAMA 308:1237–1245
38. Vavere A, Simon G, George R et al (2011) Diagnostic performance of combined noninvasive coronary angiography and myocardial perfusion imaging using 320 row detector computed tomography: design and implementation of the CORE320 multicenter, multinational diagnostic study. J Cardiovasc Comput Tomogr 5:370–381
39. Bottcher M, Refsgaard J, Madsen M et al (2003) Effect of antianginal medication on resting myocardial perfusion and pharmacologically induced hyperemia. J Nucl Cardiol 10:345–352
40. Zoghbi G, Dorfman T, Iskandrian A (2008) The effects of medications on myocardial perfusion. J Am Coll Cardiol 52:401–416
41. Koepfli P, Wyss C, Namdar M et al (2004) Beta-adrenergic blockade and myocardial perfusion in coronary artery disease: differential effects in stenotic versus remote myocardial segments. J Nucl Med 45:1626–1631